

Wavelet pressure reactivity index: a validation study

Xiuyun Liu^{1,2}, PhD, Marek Czosnyka^{1,3}, PhD, Joseph Donnelly^{1,4}, PhD, Danilo Cardim¹, PhD, Manuel Cabeleira¹, MSc, Peter J. Hutchinson¹, PhD, Xiao Hu², PhD, Peter Smielewski¹, PhD, and Ken Brady⁵, MD

1. Brain Physics Laboratory, Division of Neurosurgery, Department of Clinical Neurosciences, Addenbrooke's Hospital, University of Cambridge, Cambridge, UK
2. Department of Physiological Nursing, UCSF, San Francisco, USA
3. Institute of Electronic Systems, Warsaw University of Technology, Poland
4. Department of Anaesthesiology, University of Auckland, Auckland, New Zealand
5. Baylor College of Medicine, Houston, TX, USA

Xiuyun Liu received her B.S. and M.S. in Biomedical Engineering from Tianjin University (China) in 2009 and 2012, respectively. She received her Ph.D. degree in Clinical Neurosciences from University of Cambridge (UK) in 2017. She joined the department of physiological nursing at University of California, San Francisco, as a postdoctoral researcher in 2017. Her research focuses on cerebral autoregulation assessment, physiological signal processing, intracranial waveform analysis, biomedical models and has a particular interest in cerebral blood flow dynamics.

Dr Smielewski and Dr. Brady share joint senior authorship

Corresponding author: Xiuyun Liu

Brain Physics Laboratory, Division of Neurosurgery, Department of Clinical Neurosciences, Addenbrooke's Hospital, University of Cambridge, Hills Road, Cambridge CB2 0QQ, UK

Fax: +44 (0) 1223 216926, Tel: +44 (0) 1223 336946, e-mail: xl334@cam.ac.uk

Tables & Figures: 7

Word count: 4762

Words in abstract: 242, **words in introduction:** 759, **words in discussion:** 1129

Running head: Wavelet pressure reactivity index

Key Points

- The brain is vulnerable to damage from too little or too much blood flow. A physiological mechanism called cerebral autoregulation (CA) exists to maintain stable blood flow even if cerebral perfusion pressure (CPP) is changing.
- A robust method for assessing CA is not yet available. There are still some problems with the traditional measure, the pressure reactivity index (PRx).
- We introduced a new method, wavelet transform method (wPRx) to assess CA using data from two sets of controlled hypotension experiments in piglets: One set with artificially manipulated ABP oscillations; the other group were spontaneous ABP waves.
- A significant linear relationship was found between wPRx and PRx in both groups, with wPRx rendering a more stable result for the spontaneous waves.
- Although both methods showed similar accuracy in distinguishing intact and impaired CA, it seems that wPRx tend to perform better than PRx, though not significantly.

Abstract

We present a novel method to monitor cerebral autoregulation (CA) using the wavelet transform (WT). The new method is validated against the pressure reactivity index (PRx) in two piglet experiments with controlled hypotension. The first experiment (n=12) had controlled haemorrhage with artificial stationary arterial blood pressure (ABP) and intracranial pressure (ICP) oscillations induced by sinusoidal slow changes in positive end-expiratory pressure ('PEEP group'). The second experiment (n= 17) had venous balloon inflation during spontaneous, non-stationary ABP and ICP oscillations ('non-PEEP group'). Wavelet transform phase shift (WTP) between ABP and ICP was calculated in the frequency 0.0067 – 0.05 Hz. Wavelet semblance, the cosine of WTP was used to make the values comparable to PRx, and the new index was termed wavelet pressure reactivity index (wPRx). The traditional PRx, the running correlation coefficient between ABP and ICP, was calculated. The result showed a significant linear relationship between wPRx and PRx in the PEEP group (R = 0.88) and non-PEEP group (R= 0.56). In non-PEEP group, wPRx showed better performance than PRx in distinguishing CPP above and below lower limit of autoregulation (LLA). When CPP was decreased below LLA, wPRx increased from 0.43 ± 0.28 to 0.69 ± 0.12 ($p=0.003$) while PRx increased from 0.07 ± 0.21 to 0.27 ± 0.37 ($p=0.04$). Moreover, wPRx rendered a more stable result than PRx (SD of PRx was 0.40 ± 0.07 , and SD of wPRx was 0.28 ± 0.11 , $p= 0.001$). Assessment of CA using wavelet derived phase shift between ABP and ICP is feasible.

Key Words

cerebral autoregulation, experimental hypotension, low limit of autoregulation, pressure reactivity index, wavelet transform

Introduction

Cerebral autoregulation (CA) refers to the ability of cerebrovascular resistance to follow low frequency ($<0.05\text{Hz}$) changes in cerebral perfusion pressure (CPP) to keep cerebral blood flow (CBF) constant (Kvandal *et al.*, 2013). It is a universal physiological mechanism, depicted by the Lassen curve, with intact autoregulation delimited by lower limit of autoregulation (LLA) and upper limit of autoregulation (ULA)(Lassen, 1959; Lassen & Agnoli, 1972). Dysfunction of CA has been reported in pathologies such as stroke, traumatic brain injury, various brain lesions, infections etc., and such dysfunction may influence the patient outcomes(Paulson OB *et al.*, 1990; Tarumi *et al.*, 2014; Addison, 2015a; Kenosi *et al.*, 2015; Liu *et al.*, 2016). It is important therefore to have an effective tool for assessment and monitoring of CA.

The interrelation between arterial blood pressure (ABP), intracranial pressure (ICP) and cerebral arterial blood flow velocity (FV) provides information about functioning of CA(Aaslid *et al.*, 1986; Shigemori *et al.*, 1989; Giller, 1990; Chan *et al.*, 1992; Schmidt *et al.*, 1999; de Jong *et al.*, 2017). Invention of the pressure reactivity index (PRx), calculated as a moving correlation coefficient between ABP and ICP, has allowed for continuous monitoring of CA over extended periods of time (Czosnyka *et al.*, 1997). Negative PRx values reflect a reduction in ICP in response to an increase in ABP indicating intact CA, whereas positive PRx values, conversely, indicate impaired CA(Muizelaar *et al.*, 1989; Lang & Chesnut, 1995). Due to the fact that ICP and ABP are two commonly measured modalities in traumatic brain injury patients in intensive care unit and that no external ABP manipulations are necessary, PRx has become widely accepted as a marker for cerebral autoregulatory status (Lang *et al.*, 2015). However, PRx, being a simple correlation coefficient, is noisy due to its indiscriminant nature and inherent, incoherent, physiologic

variability of ABP and ICP (Diedler *et al.*, 2011; Brady *et al.*, 2012). Transfer function analysis approach and other frequency methods have also been developed to assess CA (Tzeng *et al.*, 2012; Tzeng & Ainslie, 2014; Tian *et al.*, 2016; Labrecque *et al.*, 2017; Chi *et al.*, 2018; van der Scheer *et al.*, 2018). However, these methods are based on the assumptions of linearity and stationarity (i.e. time invariance of statistical properties) of transmission between input (ABP) and output (cerebral blood flow, velocity or volume) of the autoregulation system.

With the clarification of the non-stationarity and non-linearity of CA (Panerai *et al.*, 1999; Panerai, 2014), attempts are being motivated to perform more sophisticated analyses to quantify the coupling mechanism of ABP and cerebral blood flow (Placek *et al.*, 2017). The wavelet transform method, is a powerful mathematical tool for analyzing intermittent, noisy, and non-stationary signals, such as measured in studies of the autonomic nervous system (Pichot *et al.*, 1999; Addison, 2002; Davrath *et al.*, 2003; Keissar *et al.*, 2009), making it also a natural candidate for assessing cerebral pressure reactivity (Bishop *et al.*, 2012; Garg *et al.*, 2014; Tian *et al.*, 2016; Chalak & Zhang, 2017; Chalak *et al.*, 2017; Wszedybyl-Winklewska *et al.*, 2017). One advantage of wavelet analysis is the ability to reveal signal features with the right balance of the temporal and frequency resolution, appropriate to the frequencies studied. The two parameters typically extracted from wavelet analysis are the wavelet phase shift (WTP), which produces maps of the localised delay (phase difference) between the two signal components over a range of frequencies and time points (Addison, 2015*b*); and the wavelet transform coherence (WTC), which characterises time and frequency dependent (cross-) correlations between those two signals (Grinsted *et al.*, 2004). A value of WTC = 1 indicates entirely linear transmission of power between two time series at a certain time and frequency point, while a value of WTC = 0, signifies no such association (Rowley *et al.*, 2007;

Kvandal *et al.*, 2013). Enforcing a certain minimal threshold of WTC can be used to find correlated areas in the time-frequency map and improve reliability (decreasing variance) of phase estimation (Grinsted *et al.*, 2004).

In this study, we have set out to apply wavelet transform analysis to assessment of CA using ABP and ICP signals and to validate the algorithm through two groups of experimental piglet data: one group with induced, sinusoidal, regular ABP waves(Brady *et al.*, 2012) and the other with spontaneous ABP waves(Brady *et al.*, 2008). The two specific objectives of the study were: 1. to validate the new method for CA assessment in conditions of high powered, regular, periodic waves of ABP (high signal to noise scenario); and 2. to establish advantages and disadvantages of the wavelet method vs. the traditional, well-established parameter, PRx.

Methods

Ethical approval

Two separate piglet models were analyzed in this study. In the first study, with induced, sinusoidal ABP waves, 12 subjects were approved by the Institutional Animal Care and Use Committee of Baylor College of Medicine (Brady *et al.*, 2012). In the other study, with spontaneous ABP waves, 17 subjects were approved by Johns Hopkins Animal Care and Use Committee(Brady *et al.*, 2008). Both animal experiments were performed in accordance with the laws of the United States of America (under animal protocol numbers 1010 and 1046) and the ethical standards mandated by the Journal of Physiology (Grundy, 2015) .Both studies conformed fully to the standards of animal experimentation described in the Guide for the Care and Use of Laboratory Animals, Eighth Edition (National Research Council), including sourcing of the animals, their preoperative care and housing, access to water and food, anesthesia and euthanasia protocols (Institute for Laboratory Animal Research, 2011).

Experimental piglets

Piglets (domestic swine, weight: 1.0-5.0 kg, Keeling Center for Comparative Medicine and Research at the University of Texas, M.D. Anderson Cancer Center, Bastrop, TX, USA) arrived at 1-2 days of age and were housed in stainless steel cages in temperature and light controlled rooms (room temperature 84-88 F, humidity 30-70%, normal light cycle: on at 7:00am off at 7:00pm). Cages were changed and cleaned daily by staff. The cages had supplemental warmth provided by water circulating heated blanket. Pigs were feed pig replacement formula ad libitum. The pigs were weighed daily to verify growth and weight gain. Bottle feeding was added if the piglets lost weight. They were taught to drink from automatic water (Birthright formula) feeder on the day they arrived and were housed in pairs to reduce stress. Piglets were acclimated for at least 24 hours prior to surgery. The model necessitates the use of very young piglets, no more than 4-5 days of age because the neonatal piglet brain develops at least 20 times faster than a human (Gressens *et al.*, 2008). Piglets were nothing by mouth (NPO) for 8 hrs before surgery to reduce the risk of reflux or vomiting on induction. The piglets were euthanized while under complete sedation with a pharmaceutical grade euthanasia solution IV before any brain harvesting or tissue removal is performed at the end of the study.

ABP wave manipulated group

Current PRx estimation is noisy due to presence of incoherent, physiologic variability of mean ABP and ICP (Diedler *et al.*, 2011; Brady *et al.*, 2012). This is likely, at least partially, due to influence of intracranial sources of variation in cerebral blood volume, not directly related to ABP, in conditions of low power slow waves in the latter. In order to minimize influences of those incoherent covariates that are not related with CA, we firstly analysed a data set from a piglet model with induced high amplitude slow waveforms in ABP (Brady *et*

al., 2012). Such controlled ABP waves provoke coherent changes in blood volume and thus ICP, improving stability of PRx calculation and making the time series of PRx considerably less noisy.

This data set included recordings from 12 piglets, in which regular, sinusoidal (1 minute period), strong ABP oscillations were induced using modulated positive end-expiratory pressure (PEEP) during volume-controlled ventilation (Brady *et al.*, 2012). The subjects were anesthetized with isoflurane, intubated by tracheotomy, and maintained under 0.8% isoflurane, 50% nitrous oxide, and 50% oxygen. Fentanyl was infused at $50 \text{ mcg}\cdot\text{kg}^{-1}\cdot\text{h}^{-1}$ carried by 0.45 normal saline with 5% dextrose and 50 Meq/l sodium bicarbonate added at $4 \text{ cc}\cdot\text{kg}^{-1}\cdot\text{h}^{-1}$. Femoral arterial and venous cannulation was performed bilaterally. ABP and central venous pressure (CVP) were transduced with a clinical monitor (GE Healthcare, Little Chalfont, UK). Craniotomy was performed for placement of an external ventricular drain, transduced as a fluid-filled column. Additional craniotomies were performed over each parietal cortex for placement of bilateral laser Doppler probes (Moor Instruments, Devon, UK). The laser Doppler probe tips were juxtaposed to the underlying cortex. The drain and probes were secured in place with dental cement. Subjects were given 20 cc/kg normal saline and recovered from surgery for 30 min while maintained under general anesthesia at normothermia (38–39°C) with arterial blood gas measurements of pH 7.37–7.43, pCO₂ 38–42 mmHg, and pO₂ 150–200 mmHg. A customized ventilator was used (Impact Instrumentation, West Caldwell, NJ). A primary wave component was applied for ventilation, which was a fixed tidal volume of 50 cm³ (cubic centimeter) at a rate between 15 and 25 per minute. Volume control ventilation prevented changes in minute ventilation with varying PEEP. A secondary slow wave component was introduced into the PEEP control. PEEP was oscillated between 5 and 10 cmH₂O in a sine-wave pattern with a period of 60 s. Once stable

recording was obtained, the piglets were hemorrhaged by syringe-pump withdrawal at a rate of 12% calculated blood vol/h, which allowed the procedure of gradual ABP reduction over 3-4 hours before demise. For later analysis, this group was labelled PEEP Group. The data has been published as part of a validation study of the pressure-reactivity index (Brady *et al.*, 2012).

Spontaneous ABP wave group

After the validation study using 'PEEP' data set described above, a comparison between the wavelet method and traditional PRx was conducted in a more clinically relevant setting of spontaneous ABP waves at two ICP levels: naïve (ICP= 10 mmHg, n=10) and elevated ICP (ICP= 20 mmHg, n=7). For the wavelet based PRx and traditional PRx, the stability and the ability of distinguishing CPP above LLA (indicating good CA) and below LLA (indicating bad CA) was compared.

After tracheostomy and mechanical ventilation (goal pH, 7.35–7.45; pO₂, 200–300 mm Hg, pCO₂, 35–45), the 17 infant piglets were anesthetized with isoflurane, intubated by tracheotomy, and maintained under 0.8% isoflurane, 50% nitrous oxide, and 50% oxygen combined with IV dosing of vecuronium (5 mg bolus and 2 mg/h infusion) and fentanyl (25 µg bolus and 25 µg/h infusion). Warming pads were applied to maintain brain and rectal temperature at 38.5–39.5°C. For the 7 piglets with elevated ICP, artificial cerebrospinal fluid (KCl 3.0 mmol/L, MgCl₂ 0.6 mmol/L, CaCl₂ 1.3 mmol/L, NaCl 131.8 mmol/L, NaHCO₃ 24.6 mmol/L, urea 6.7 mmol/L, and glucose 3.6 mmol/L) was infused in an external ventricular drain catheter at varying rates to achieve and maintain a steady-state ICP of ≈20 mm Hg throughout the experiment (Brady *et al.*, 2008, 2009).

Once the piglets were anesthetized, a central venous line and a 5 Fr esophageal balloon catheter (Cooper Surgical, Trundall, CT) were placed in the femoral veins. Gradual inflation of the balloon catheter by infusion of saline from a syringe pump at the level of the inferior vena cava was the mechanism of inducing hypotension in the piglets. The CPP was slowly decreased to approximately 10 mm Hg over 3 hours before demise.

The femoral artery was cannulated for placement of a pressure monitoring line. The ABP was continuously monitored after setting the transducer to zero at the level of the external auditory meatus, which was also at the level of the left atrium. For piglets in the naïve ICP group, a single external ventricular drain catheter was placed 4 mm lateral and 4 mm rostral to the bregma at midline through a 2–3 mm craniotomy. Piglets in elevated ICP group required an additional contralateral 2–3 mm craniotomy for placement of a second external ventricular drain for a CSF infusion. Continuous ICP was monitored by transduction of the external ventricular drain in all animals with pressure lines set to zero at the external auditory meatus. Craniotomy was also performed 4 mm lateral and 4 mm rostral to the first craniotomy in all piglets for placement of a laser Doppler probe (Moor Instruments, Devon, UK), positioned against the surface of the frontoparietal cortex. Craniotomies were sealed with dental cement. Later, this group was labeled non-PEEP Group. The data of spontaneous waves have been used to test the lower limit of cerebral autoregulation(Brady *et al.*, 2008, 2009).

Data collection

In both experiments, ABP, ICP, and CBF were monitored continuously. ABP was transduced invasively with a clinical monitor (Marquette Solar 8000, GE Healthcare, Little Chalfont, UK). ICP was monitored through an external ventricular drain after craniotomy. Bilateral laser Doppler probes (Moor Instruments, Devon, UK) were placed to monitor CBF after

additional craniotomies over each parietal cortex. The signals were all sampled at 200 Hz, digitized using an A/D converter (DT9801, Data Translation, Marlboro, MA), and were recorded using a laptop computer with ICM+® software (Cambridge Enterprise Ltd, Cambridge, UK, <http://icmplus.neurosurg.cam.ac.uk>). The same software was later used for the retrospective analysis of all stored signals.

Data Analysis

Wavelet Semblance (wPRx)

Wavelet transform phase shift (WTP) between ABP and ICP in the low frequency range of 0.0067 Hz to 0.05 Hz was calculated through complex, continuous wavelet transform (Torrence & Compo, 1998; Highton *et al.*, 2015; Tian *et al.*, 2016; Liu *et al.*, 2017a). In brief, the WTP at each scale-frequency point was calculated from 500 seconds long data segments (moving window, with update every 10 seconds), and subsequently wavelet transform coherence (WTC) was used to reject corresponding unreliable phase values. In this paper, the WTC threshold of 0.48 was used, determined through 10000 Monte Carlo simulations approach (detailed description can be found in a previously published paper(Liu *et al.*, 2017a)). Individual phase shift values with coherence higher than 0.48 were kept, while data points with coherence lower than the threshold were deleted. Wavelet semblance(Cooper & Cowan, 2008), which is cosine of wavelet phase shift was calculated, and labelled wavelet pressure reactivity index (wPRx). Finally the values were averaged along the frequency domain, resulting in one wPRx value at each time point. A 500-second window length was chosen as an attempt to make it comparable to the standard PRx calculation period of 300 seconds but accounting for edge effects of the wavelet transform(Addison, 2002, 2016). The application of wavelet semblance limits wPRx range from -1 (180 degrees phase shift, inversely correlated) through 0 (uncorrelated) to +1 (0 degrees phase shift, fully and

positively correlated), rendering a metric with direct correspondence to PRx(Cooper & Cowan, 2008). In addition, the cosine operation offers a practical solution to the problem of phase wrapping, as in effect the value obtained is equal to the normalized real part of the wavelet transfer function, and therefore not subject to the wrapping effects.

Determining the Lower Limit of Autoregulation

In both experiments, CPP was gradually decreased either through syringe-pump withdraw (PEEP group) or through a balloon catheter (non-PEEP wave) until values of CPP well below the lower limit of autoregulation (LLA) were reached. Each subject's LLA was determined through a scatter plot of 1-minute average Laser Doppler flow versus CPP(Brady *et al.*, 2008; Lee *et al.*, 2009). The CPP value at the left intersection of 2 lines defined by a piecewise linear regression model was defined as LLA (Fig.1). The ability of wPRx and PRx in distinguishing CPP above LLA and below LLA was compared.

Pressure Reactivity Index (PRx)

The PRx was calculated according to previously published methods(Czosnyka *et al.*, 1997). First, ABP and ICP are filtered to remove pulse and respiratory frequency waveforms with 10 second averaging. A moving Pearson correlation coefficient of 30 consecutive samples (300 seconds) renders the standard PRx(Czosnyka *et al.*, 1997). All the abbreviations were summarized in Table 1.

Statistics

SPSS software (version 21, IBM, Armonk, NK,USA) was used for statistical analysis. Linear regression was used to describe relationship between PRx and wPRx. Pearson's correlation coefficient (r) was used to examine linearity of the relationship. Paired t test was used to compare the ability of PRx and wPRx in distinguishing intact CA (CPP above LLA) and

impaired CA (CPP below LLA). A receiver-operator characteristic (ROC) test was also done, rendering an area under ROC curve (AUC-ROC) for each parameter. Statistical differences between AUC-ROC curves were verified using the DeLong's test for two correlated ROC curves (R package pROC)(Robin *et al.*, 2013). Bland-Altman plots were used to investigate the agreement between the two variables. Kruskal-Wallis test was used to compare the standard deviation of PRx and wPRx. Results were considered significant at $p < 0.05$.

Results

Wavelet transform calculation

A representative example of wavelet phase shift and wavelet coherence between ABP and ICP from a single experimental dataset (PEEP group) is shown in Fig.2. While ABP was gradually decreased (Fig.2A), wavelet phase shift showed a synchronized decrease at the frequency of 1/min (PEEP wave frequency), demonstrated by the color change from red to blue in Fig.2C. This phase shift change from roughly 3 radians (red) to less than one radian (blue) is interpreted as the transition from intact CA to impaired CA due to CPP below LLA. Phase semblance result was shown in Fig. 2D. In this protocol, the wavelet coherence in the same frequency remained stable and high across the whole period, shown by red color (Fig.2E). Fig.2F showed the average value of coherence across the whole frequency range at each time point, and it was clear that for this sample, the frequency-averaged WTC was mostly above the threshold level of 0.48.

The relationship between wPRx and PRx

Relationship between wPRx and PRx was analyzed using 30-minute average values (n=118 in PEEP group, n=262 in non-PEEP group, Fig.3). wPRx was positively related with PRx and PRx in PEEP group ($R=0.88$, Fig.3A) and non-PEEP group ($R=0.56$, Fig.3C). The Bland

Altman chart showed a tendency of a negative PRx-wPRx difference (Fig. 3B and Fig.3D). The mean difference between PRx and wPRx was -0.23 (95% CI: -0.64 ~ 0.18) in PEEP group and -0.4 (95% CI: -0.91~0.11) in non-PEEP group.

Stability of PRx and wPRx

Stability of the two parameters was compared through mean standard deviation when CPP was above LLA. Because of the induced regular ABP oscillations, there was no difference between PRx and wPRx in PEEP group (SD of PRx = 0.47 ± 0.06 , SD of wPRx = 0.48 ± 0.07 , n=12, p>0.05). However, the advantage of wPRx was demonstrated in the spontaneous non-PEEP group, with smaller SD of wPRx (SD of PRx was 0.40 ± 0.07 , and SD of wPRx was 0.28 ± 0.11 , p= 0.001).

Comparing wPRx and PRx against LLA in PEEP Group

The average LLA of the PEEP group was 33.75 mm Hg (95% CI: 27.6–39.9 mmHg), and average LLA of non-PEEP group was 36.4 mm Hg (95% CI: 29.5 – 43.2 mmHg). Fig.4 displayed an example of averaged PRx and wPRx in (CPP-LLA) bins. Both PRx and wPRx were increased significantly while CPP was decreased below LLA, indicating worse autoregulation.

In PEEP group, mean PRx increased significantly from -0.22 ± 0.33 to 0.41 ± 0.20 (p<0.001, Fig.5A) and wPRx increased from -0.02 ± 0.35 to 0.58 ± 0.21 (p<0.001, Fig.5B) while CPP was decreased below LLA. In non-PEEP group, wPRx showed more significant increase (from 0.43 ± 0.28 to 0.69 ± 0.12 , p=0.003, Fig.5D) than PRx (from 0.07 ± 0.21 to 0.27 ± 0.37 , p=0.04, Fig.5C).

AUC-ROC curve showed that both wPRx and PRx can differentiate CPP above or below LLA (Fig.6). In PEEP wave, AUC-ROC of PRx and wPRx were 0.94 (95% CI: 0.76-1) and 0.96 (95% CI: 0.79-1) respectively. In non-PEEP wave, AUC-ROC of PRx and wPRx were

0.73 (95% CI:0.55-0.87) and 0.83 respectively (95% CI: 0.66-0.93) though, possibly because of small N, the DeLong's test showed no significant difference between the two AUC-ROC curves of PRx and wPRx in both groups.

Discussion

Because cerebral slow-wave activity is generally non-periodic and nonstationary, it poses a challenge for traditional, Fourier based signal-processing techniques. The wavelet technique, well suited to this type of signals, has previously been described in several studies for cerebral autoregulation assessment (Latka *et al.*, 2005; Peng *et al.*, 2010; Highton *et al.*, 2015; Tian *et al.*, 2016; Chalak & Zhang, 2017; Chalak *et al.*, 2017; Liu *et al.*, 2017a). In this paper, we have applied wavelet semblance algorithm firstly in two piglet experiments and used wavelet coherence as a guard of a reliable ABP-ICP phase relationship. The main finding was that wPRx produced more stable result than PRx and could distinguish CPP above and below LLA more significantly when spontaneous ABP and ICP waves were analysed.

Validation of wPRx

In order to validate the wavelet method against the well-established PRx index, this study used a piglet model with regular ABP oscillations by adding sinusoidal variations in PEEP during volume-controlled ventilation (Brady *et al.*, 2009, 2012). This significantly improved stability (lowered variance) of PRx and therefore wPRx was not expected to perform any better than PRx, as the strong, deterministic component of approximately fixed frequency and amplitude induced in ABP removed any advantages of a non-stationary approach. However, the resulting strong linear relationship between the two parameters validated wPRx principle. As wPRx directly reflects phase shift between ABP and ICP, this result provides an evidence that high positive PRx values reflect near 0 phase shift (cosine close to 1) between ABP and

ICP (that is completely impaired autoregulation), while negative values of PRx correspond to highly positive phase shifts (90° to 180° , negative cosine, highly active autoregulation).

The potential advantages of wPRx lie in dealing with spontaneous waves in ABP of varying intensity and frequency. Transmission of these variable waves into the output signal (ICP) waveforms may be partially masked by other independent (intracranial) sources of fluctuations in ICP, thus making PRx less reliable (noisy), because of its indiscriminant nature. These circumstances will also lead to reduced coherence between ABP and ICP. Thus using coherence as a filter should produce more stable result, and that was indeed demonstrated by increased stability of the wPRx in non-PEEP group.

Wavelet analysis

The wavelet transform expands time series into a time-frequency space with desired temporal-frequency resolution, to fit various needs for non-stationary signal analysis (Grinsted *et al.*, 2004). In his review, Smith discussed the use of wavelet-based techniques to aid the interpretation of complex time-variant signals by producing qualitative and quantitative evidence of cerebrovascular autoregulation that is otherwise ‘not possible using other methods’ (Smith, 2011; Addison, 2015a). The Morlet wavelet, a complex function, is a natural choice when phase feature extraction is needed. Coherence (in this case WTC) threshold is often used to ensure a reliable estimate of phase relationship between input and output. This combination of wavelet derived instantaneous phase accompanied by coherence derived quality control makes it, in general, a more robust method for non-stationary signal analysis.

However, defining an appropriate threshold for coherence is generally not trivial as it will vary depending on the values of various parameters of the estimation process (Faes *et al.*, 2004). Therefore we chose to establish that threshold using Monte Carlo simulations in which

surrogates of ABP and ICP with destroyed phase relationship were generated and analyzed. As ultimately the method needs to be applicable to real-time analysis, and given that Monte Carlo simulations carry a significant performance penalty, we chose to calculate a single threshold for the whole dataset, rather than estimating it for each individual recording. Reassuringly this threshold matched our previous result in a large cohort of TBI patients(Liu *et al.*, 2017a).

Thus said, it must be acknowledged that there may be a considerable variability of coherence threshold in different acute brain injury patients (Highton *et al.*, 2015), because of the differences in autocorrelation in individual datasets. Ideally therefore an individual coherence threshold should be considered in the future.

Wavelet transform coherence

Wavelet transform coherence (WTC) characterizes cross-correlations between two signals. A value of WTC close to 1 indicates a high common power (more precisely highly correlated variability in power) between two time series at a certain time and frequency area, and it guarantees linear relationships between two signals at that point in time and frequency (and thus a reliably estimation of phase at that point). On the other hand a low value of WTC, shows a vanishing correlation, possibly caused by external noise or a non-linear relationship(Zhang *et al.*, 1998). In case of transmission between ABP and cerebral blood flow, it can also be argued that coherence per se could be an indicator of CA, with high coherence indicating impaired CA (slow variations in ICP are linearly and passively related to slow variations in ABP), and low coherence indicating properly functioning CA because of the strong fluctuations attenuating (and possibly non-linear) effect of CA (Giller, 1990; Zhang *et al.*, 1998). Rejecting low coherence as "noise" may therefore dismiss areas that still contain valid information about CA and in effect this may lead to disproportionately low

sampling from regions of intact autoregulation. As a result fewer semblance values will contribute to final summary (mean) value, potentially increasing its variance. However our results showed overall improvement of stability of wPRx over PRx, thus suggesting good balance between removing seemingly uncorrelated data points and decreasing valid data points count for averaging. Additionally the apparent better ability of wPRx, with the coherence mask, to distinguish CPP above and below LLA is reassuring.

Potential clinical usage

PRx has been used for estimation of the optimal, or safe range of CPP for patients with TBI(Donnelly *et al.*, 2017; Liu *et al.*, 2017b) . Deviation from optimal CPP defined by PRx monitoring is associated with death and permanent neurologic disability(Aries *et al.*, 2012). Maintenance of CPP at the optimal range defined by PRx monitoring is associated with the highest rate of survival with intact neurologic function. However, it is known that the PRx can be imprecise, due to transient fluctuations in the ABP and ICP signals unrelated to autoregulation. This imprecision necessitates prolonged time windows to delineate optimal CPP reliably. 4 hours is agreed minimal period for estimation of optimal CPP(Aries *et al.*, 2012), and so far there is no evidence that shorter windows are feasible. Also, the yield of optimal CPP is not high (around 50%) using PRx (Aries *et al.*, 2012; Depreitere *et al.*, 2014). Improvements of the precision of PRx monitoring have the potential to improve the optimal CPP yield and this has been shown in a recent publication(Liu *et al.*, 2017a). The use of wavelet transform with coherence filtering, as demonstrated in this study is a viable method to improve the signal to noise ratio, and have the potential to improve optimal CPP yield for future clinical usage.

Conclusion

In this study, a new wavelet-transform-based method, suitable for non-stationary signals, was introduced to assess CA. The new method, termed wavelet transform pressure reactivity index (wPRx) was validated through two groups of experimental piglets' data. The results showed a strong, linear relationship and high agreement between wPRx and the time-correlation-based index, PRx. Both PRx and wPRx can distinguish CPP above and below LLA, while wPRx demonstrated more stable results than PRx.

References

- Aaslid R, Lundar T, Lindegaard KF & Nornes H (1986). Estimation of Cerebral Perfusion Pressure from Arterial Blood Pressure and Transcranial Doppler Recordings. *Intracranial Press* VI226–229.
- Addison PS (2002). *The Illustrated Wavelet Transform Handbook: Introductory Theory and Applications in Science, Engineering, Medicine and Finance 1st Edition*. CRC Press, Boca Raton.
- Addison PS (2015a). A Review of Wavelet Transform Time-Frequency Methods for NIRS-based Analysis of Cerebral Autoregulation. *IEEE Rev Biomed Eng* **PP**, 1.
- Addison PS (2015b). Identifying stable phase coupling associated with cerebral autoregulation using the synchrosqueezed cross-wavelet transform and low oscillation morlet wavelets. *Conf Proc IEEE Eng Med Biol Soc* **8**, 5960–5963.
- Addison PS (2016). *The Illustrated Wavelet Transform Handbook: Introductory Theory and Applications in Science, Engineering, Medicine and Finance, Second Edition*. CRC Press, Taylor & Francis Group, Boca Raton.
- Aries MJH, Czosnyka M, Budohoski KP, Steiner L a., Lavinio A, Koliass AG, Hutchinson PJ,

- Brady KM, Menon DK, Pickard JD & Smielewski P (2012). Continuous determination of optimal cerebral perfusion pressure in traumatic brain injury. *Crit Care Med* **40**, 2456–2463.
- Bishop SM, Yarham SI, Navapurkar VU, Menon DK & Ercole A (2012). Multifractal analysis of hemodynamic behavior: intraoperative instability and its pharmacological manipulation. *Anesthesiology* **117**, 810–821.
- Brady KM, Easley RB, Kibler K, Kaczka DW, Andropoulos D, Fraser CD, Smielewski P, Czosnyka M, Adams GJ, Rhee CJ & Rusin CG (2012). Positive end-expiratory pressure oscillation facilitates brain vascular reactivity monitoring. *J Appl Physiol* **113**, 1362–1368.
- Brady KM, Lee JK, Kibler KK, Easley RB, Koehler RC, Czosnyka M, Smielewski P & Shaffner DH (2009). The lower limit of cerebral blood flow autoregulation is increased with elevated intracranial pressure. *Anesth Analg* **108**, 1278–1283.
- Brady KM, Lee JK, Kibler KK, Easley RB, Koehler RC & Shaffner DH (2008). Continuous measurement of autoregulation by spontaneous fluctuations in cerebral perfusion pressure: comparison of 3 methods. *Stroke* **39**, 2531–2537.
- Chalak L, Tian F, Adams-Huet B, Vasil D, Laptook A, Tarumi T & Zhang R (2017). Novel Wavelet Real Time Analysis of Neurovascular Coupling in Neonatal Encephalopathy. *Sci Rep*; DOI: 10.1038/srep45958.
- Chalak LF & Zhang R (2017). New Wavelet Neurovascular Bundle for Bedside Evaluation of Cerebral Autoregulation and Neurovascular Coupling in Newborns with Hypoxic-Ischemic Encephalopathy. *Dev Neurosci* **39**, 89–96.
- Chan KH, Miller JD, Dearden NM, Andrews PJ & Midgley S (1992). The effect of changes in cerebral perfusion pressure upon middle cerebral artery blood flow velocity and jugular bulb venous oxygen saturation after severe brain injury. *J Neurosurg* **77**, 55–61.

- Chi N, Wang C, Chan L & Hu H (2018). Comparing Different Recording Lengths of Dynamic Cerebral Autoregulation: 5 versus 10 Minutes. *Biomed Res Int*; DOI: <https://doi.org/10.1155/2018/7803426>.
- Cooper GRJ & Cowan DR (2008). Comparing time series using wavelet-based semblance analysis. *Comput Geosci* **34**, 95–102.
- Czosnyka M, Smielewski P, Kirkpatrick P, Laing RJ, Menon D & Pickard JD (1997). Continuous assessment of the cerebral vasomotor reactivity in head injury. *Neurosurgery* **41**, 11–19.
- Davrath LR, Goren Y, Pinhas I, Toledo E & Akselrod S (2003). Early autonomic malfunction in normotensive individuals with a genetic predisposition to essential hypertension. *Am J Physiol Heart Circ Physiol* **285**, H1697-704.
- Depreitere B, Güiza F, Van den Berghe G, Schuhmann MU, Maier G, Piper I & Meyfroidt G (2014). Pressure autoregulation monitoring and cerebral perfusion pressure target recommendation in patients with severe traumatic brain injury based on minute-by-minute monitoring data. *J Neurosurg* **120**, 1451–1457.
- Diedler J, Zweifel C, Budohoski K, Kasprowicz M, Sorrentino E, Haubrich C, Brady K, Czosnyka M, Pickard J & Smielewski P (2011). The limitations of near-infrared spectroscopy to assess cerebrovascular reactivity: the role of slow frequency oscillations. *Anesth Analg* **113**, 849–857.
- Donnelly J, Czosnyka M, Adams H, Robba C, Steiner LA, Cardim D, Cabella B, Liu X, Ercole A, Hutchinson PJ, Menon DK, Aries MJH & Smielewski P (2017). Individualizing Thresholds of Cerebral Perfusion Pressure Using Estimated Limits of Autoregulation. *Crit Care Med* **45**, 1464–1471.
- Faes L, Pinna GD, Porta A, Maestri R & Nollo G (2004). Surrogate data analysis for assessing the significance of the coherence function. *IEEE Trans Biomed Eng* **51**, 1156–

1166.

- Garg A, Xu D, Laurin A & Blaber AP (2014). Physiological interdependence of the cardiovascular and postural control systems under orthostatic stress. *Am J Physiol Heart Circ Physiol* **307**, H259-64.
- Giller C a (1990). The frequency-dependent behavior of cerebral autoregulation. *Neurosurgery* **27**, 362–368. Available at: <http://www.ncbi.nlm.nih.gov/pubmed/2234328>.
- Gressens P, Dingley J, Plaisant F, Porter H, Schwendimann L, Verney C, Tooley J & Thoresen M (2008). Analysis of neuronal, glial, endothelial, axonal and apoptotic markers following moderate therapeutic hypothermia and anesthesia in the developing piglet brain. *Brain Pathol* **18**, 10–20.
- Grinsted a., Moore JC & Jevrejeva S (2004). Application of the cross wavelet transform and wavelet coherence to geophysical time series. *Nonlinear Process Geophys* **11**, 561–566.
- Grundy D (2015). Principles and standards for reporting animal experiments in The Journal of Physiology and Experimental Physiology. *Exp Physiol* **100**, 755–758.
- Highton D, Ghosh A, Tachtsidis I, Panovska-Griffiths J, Elwell CE & Smith M (2015). Monitoring cerebral autoregulation after brain injury: Multimodal assessment of cerebral slow-wave oscillations using near-infrared spectroscopy. *Anesth Analg* **121**, 198–205.
- Institute for Laboratory Animal Research (2011). *Guide for the Care and Use of Laboratory Animals: 8th Ed.*
- de Jong DLK, Tarumi T, Liu J, Zhang R & Claassen JAHR (2017). Lack of linear correlation between dynamic and steady-state cerebral autoregulation. *J Physiol* **595**, 5623–5636.
- Keissar K, Davrath LR & Akselrod S (2009). Coherence analysis between respiration and heart rate variability using continuous wavelet transform. *Philos Trans A Math Phys Eng Sci* **367**, 1393–1406.

- Kenosi M, Naulaers G, Ryan CA & Dempsey EM (2015). Current research suggests that the future looks brighter for cerebral oxygenation monitoring in preterm infants. *Acta Paediatr* **104**, 225–231.
- Kvandal P, Sheppard L, Landsverk SA, Stefanovska A & Kirkeboen KA (2013). Impaired cerebrovascular reactivity after acute traumatic brain injury can be detected by wavelet phase coherence analysis of the intracranial and arterial blood pressure signals. *J Clin Monit Comput* **27**, 375–383.
- Labrecque L, Rahimaly K, Imhoff S, Paquette M, Le Blanc O, Malenfant S, Lucas SJE, Bailey DM, Smirl JD & Brassard P (2017). Diminished dynamic cerebral autoregulatory capacity with forced oscillations in mean arterial pressure with elevated cardiorespiratory fitness. *Physiol Rep* **5**, 21.
- Lang EW & Chesnut RM (1995). Intracranial pressure and cerebral perfusion pressure in severe head injury. *New Horiz* **3**, 400–409.
- Lang EW, Kasproicz M, Smielewski P, Santos E, Pickard J & Czosnyka M (2015). Short pressure reactivity index versus long pressure reactivity index in the management of traumatic brain injury. *J Neurosurg* **122**, 588–594.
- Lassen N (1959). Cerebral blood flow and oxygen consumption in man. *Physiol Rev* **39**, 183–238.
- Lassen NA & Agnoli A (1972). The upper limit of autoregulation of cerebral blood flow - on the pathogenesis of hypertensive encephalopathy. *Scand J Clin Lab Invest* **30**, 113–116.
- Latka M, Turalska M, Glaubic-Latka M, Kolodziej W, Latka D & West BJ (2005). Phase dynamics in cerebral autoregulation. *Am J Physiol Heart Circ Physiol* **289**, H2272-9.
- Lee JK, Kibler KK, Benni PB, Easley RB, Czosnyka M, Smielewski P, Koehler RC, Shaffner DH & Brady KM (2009). Cerebrovascular reactivity measured by near-infrared spectroscopy. *Stroke* **40**, 1820–1826.

- Liu J, Tseng BY, Khan MA, Tarumi T, Hill C, Mirshams N, Hodics TM, Hynan LS & Zhang R (2016). Individual variability of cerebral autoregulation, posterior cerebral circulation and white matter hyperintensity. *J Physiol* **594**, 3141–3155.
- Liu X, Donnelly J, Czosnyka M, Aries MJH, Brady K, Cardim D, Robba C, Cabeleira M, Kim D-J, Haubrich C, Hutchinson PJ & Smielewski P (2017a). Cerebrovascular pressure reactivity monitoring using wavelet analysis in traumatic brain injury patients: A retrospective study. *PLOS Med* **14**, 7.
- Liu X, Maurits N, Aries M, Czosnyka M, Ercole A, Donnelly J, Cardim D, Kim D, Dias C, Cabeleira M & Smielewski P (2017b). Monitoring of optimal cerebral perfusion pressure in traumatic brain injured patients using a multi-window weighting algorithm. *J Neurotrauma* **34**, 3081–3088.
- Muizelaar J, Ward J, Marmarou A, Newlon P & Wachi A (1989). Cerebral blood flow and metabolism in severely head-injured children Part 2: Autoregulation. *J Neurosurg* **71**, 72–76.
- Panerai RB (2014). Nonstationarity of dynamic cerebral autoregulation. *Med Eng Phys* **36**, 576–584.
- Panerai RB, Dawson SL & Potter JF (1999). Linear and nonlinear analysis of human dynamic cerebral autoregulation. *Am J Physiol* **277**, H1089-99.
- Paulson OB, Strandgaard S & Edvinsson L (1990). Cerebral autoregulation. *Cerebrovasc brain Metab Rev* **2**, 161–192.
- Peng T, Rowley AB, Ainslie PN, Poulin MJ & Payne SJ (2010). Wavelet Phase Synchronization Analysis of Cerebral Blood Flow Autoregulation. *IEEE Trans Biomed Eng* **57**, 960–968.
- Pichot V, Gaspoz JM, Molliex S, Antoniadis A, Busso T, Roche F, Costes F, Quintin L, Lacour JR, Barthélémy JC, Busso T, Roche F, Costes F, Quintin L, Lacour JR &

- Barthélémy JC (1999). *Wavelet transform to quantify heart rate variability and to assess its instantaneous changes*.
- Placek MM, Wachel P, Iskander DR, Smielewski P, Uryga A, Mielczarek A, Szczepański TA & Kasprowicz M (2017). Applying time-frequency analysis to assess cerebral autoregulation during hypercapnia. *PLoS One* **12**, 7.
- Robin AX, Turck N, Hainard A, Lisacek F, Sanchez J, Müller M & Xavierrobinunigech MXR (2013). Package “pROC.” *2012-09-10 09:34:561–71*.
- Rowley a B, Payne SJ, Tachtsidis I, Ebden MJ, Whiteley JP, Gavaghan DJ, Tarassenko L, Smith M, Elwell CE & Delpy DT (2007). Synchronization between arterial blood pressure and cerebral oxyhaemoglobin concentration investigated by wavelet cross-correlation. *Physiol Meas* **28**, 161–173.
- van der Scheer J, Kamijo Y, Leicht C, Millar P, Shibasaki M, Goosey-Tolfrey V & Tajima F (2018). A comparison of static and dynamic cerebral autoregulation during mild whole-body cold stress in individuals with and without cervical spinal cord injury: a pilot study. *Spinal Cord*; DOI: 10.1038/s41393-017-0021-7.
- Schmidt B, Czosnyka M, Schwarze JJ, Sander D, Gerstner W, Lumenta CB, Pickard JD & Klingelhöfer J (1999). Cerebral vasodilatation causing acute intracranial hypertension: a method for noninvasive assessment. *J Cereb Blood Flow Metab* **19**, 990–996.
- Shigemori M, Nakashima H, Moriyama T, Tokutomi T, Nishio N, Harada K & Kuramoto S (1989). Noninvasive study of critical thresholds of intracranial pressure and cerebral perfusion pressure for cerebral circulation and brain function. *Neurol Res* **11**, 165–168.
- Smith M (2011). Shedding light on the adult brain: a review of the clinical applications of near-infrared spectroscopy. *Philos Trans A Math Phys Eng Sci* **369**, 4452–4469.
- Tarumi T, Dunskey DI, Khan MA, Liu J, Hill C, Armstrong K, Martin-Cook K, Cullum CM & Zhang R (2014). Dynamic cerebral autoregulation and tissue oxygenation in amnesic

- mild cognitive impairment. *J Alzheimers Dis* **41**, 765–778.
- Tian F, Tarumi T, Liu H, Zhang R & Chalak L (2016). Wavelet coherence analysis of dynamic cerebral autoregulation in neonatal hypoxic-ischemic encephalopathy. *NeuroImage Clin* **11**, 124–132.
- Torrence C & Compo GP (1998). A Practical Guide to Wavelet Analysis. *Bull Am Meteorol Soc* **79**, 61–78.
- Tzeng YC & Ainslie PN (2014). Blood pressure regulation IX: Cerebral autoregulation under blood pressure challenges. *Eur J Appl Physiol* **114**, 545–559.
- Tzeng YC, Ainslie PN, Cooke WH, Peebles KC, Willie CK, MacRae BA, Smirl JD, Horsman HM & Rickards CA (2012). Assessment of cerebral autoregulation: the quandary of quantification. *Am J Physiol Heart Circ Physiol* **303**, H658-71.
- Wszedybyl-Winklewska M, Wolf J, Swierblewska E, Kunicka K, Gruszecka A, Gruszecki M, Kucharska W, Winklewski PJ, Zabulewicz J, Guminski W, Pietrewicz M, Frydrychowski AF, Bieniaszewski L & Narkiewicz K (2017). Acute hypoxia diminishes the relationship between blood pressure and subarachnoid space width oscillations at the human cardiac frequency. *PLoS One* **12**, 2.
- Zhang R, Zuckerman JH, Giller CA & Levine BD (1998). Transfer function analysis of dynamic cerebral autoregulation in humans. *Am J Physiol* **274**, 233–241.

Additional information section**Competing Interests**

ICM+ Software is licensed by Cambridge Enterprise, Cambridge, UK, (<http://icmplus.neurosurg.cam.ac.uk>). MCz and PS have a financial interest in a fraction of the licensing fee.

Author contributions

K.B. designed the animal experiment, acquired, analysed and interpreted the data and revised the manuscript. P.S., M.Cz. designed the work, interpreted the data and revised the manuscript. X.Y.L. analysed, interpreted the data and wrote the manuscript. J.D. and D.C. interpreted the data and revised the manuscript. M.Ca analysed the data and revised the manuscript. P.J.H. interpreted the data and revised the manuscript. X.H. interpreted the data and revised the manuscript. All authors have approved the final version of the manuscript and agreed to be accountable for all aspects of the work in ensuring that questions related to the accuracy or integrity of any part of the work are appropriately investigated and resolved. All persons designated as authors qualify for authorship, and all those who qualify for authorship are listed.

Funding

The authors received no specific funding for this work.

Author profile

Xiuyun Liu received her B.S. and M.S. in Biomedical Engineering from Tianjin University (China) in 2009 and 2012, respectively. She received her Ph.D. degree in Clinical Neurosciences from University of Cambridge (UK) in 2017. She joined the department of physiological nursing at University of California, San Francisco, as a postdoctoral researcher in 2017. Her research focuses on cerebral autoregulation assessment, physiological signal

processing, intracranial waveform analysis, biomedical models and has a particular interest in cerebral blood flow dynamics.

Tables

Table 1 Abbreviations used in the article

Abbreviation	Full name	Abbreviation	Full name
ABP	Arterial blood pressure	AUC-ROC	Area under receiver-operator characteristic curve
CA	Cerebral autoregulation	CBF	Cerebral blood flow
CPP	Cerebral perfusion pressure	FV	Cerebral blood flow velocity
ICP	Intracranial pressure	LLA	Lower limit of autoregulation
PEEP	positive end-expiratory pressure	PRx	Pressure reactivity index using 300-second window
ROC	Receiver-operator characteristic	ULA	Upper limit of autoregulation
wPRx	Wavelet semblance	WTC	Wavelet transform coherence
WTP	Wavelet transform phase shift		

Figure Legends

Fig. 1 Demonstration of lower limit of autoregulation (LLA) using laser Doppler cerebral blood flow (CBF) and cerebral perfusion pressure (CPP) as a breakpoint between two linear sections estimated using the least mean square distance (data from one piglet).

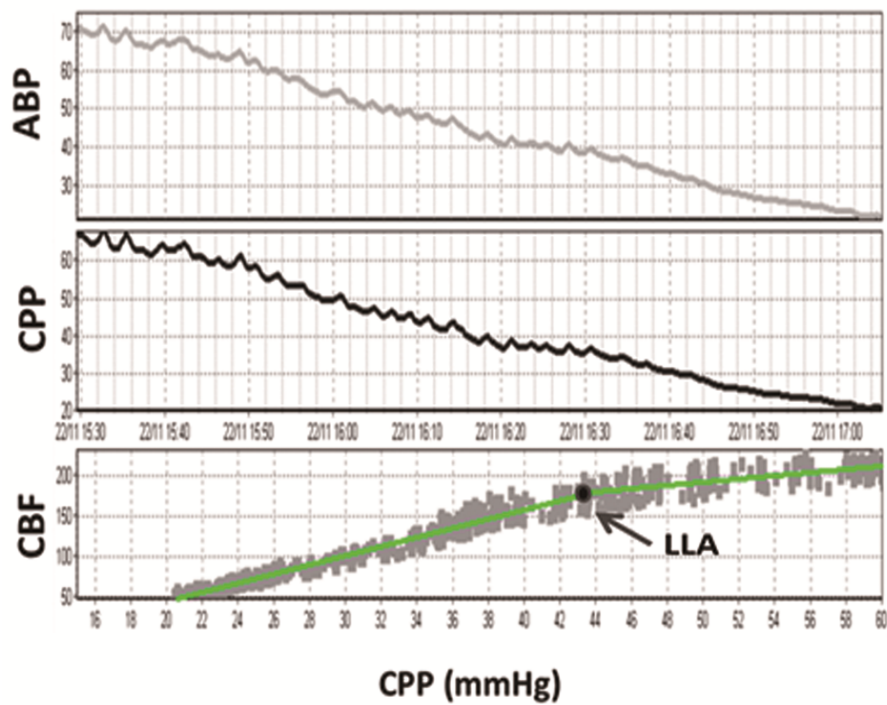


Fig.2 Changing wavelet phase (WTP), wavelet semblance and coherence (WTC) between ABP and ICP of one piglet in the PEEP group. (A) Arterial blood pressure, ABP. (B) Intracranial pressure, ICP. (C) The WTP map between ABP and ICP. Red color indicates higher value and blue color implies lower value. (D) The wavelet semblance map. (E) The WTC map. (F) The average value of WTC across the whole frequency average at each time point. The dash line is the significance level of WTC. The Morlet wavelet characteristic angular frequency $w_0=2\pi$. Wavelet semblance: cosine of wavelet phase shift.

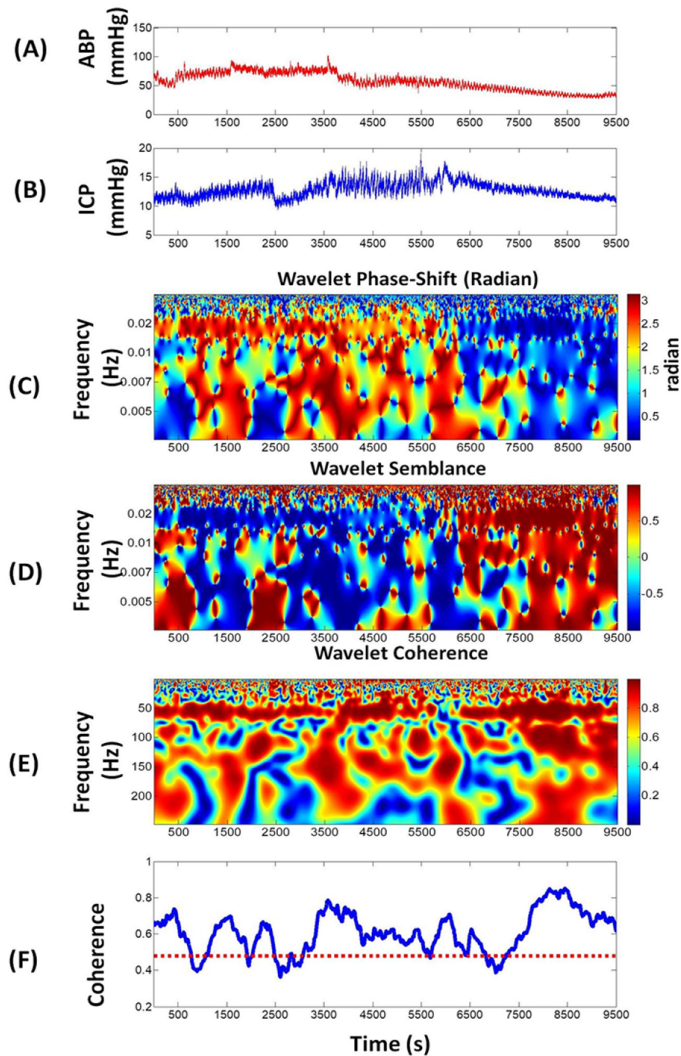


Fig.3 Relationship between PRx and wPRx in the PEEP group (A) and in the non-PEEP group (C). The Bland-Altman plot between PRx and wPRx in PEEP group (B) and in non-PEEP group (D). PRx: pressure reactivity index; wPRx: wavelet semblance; PEEP: positive end-expiratory pressure. Bland-Altman was used to analyze the agreement of the two indices. CI: confidence interval.

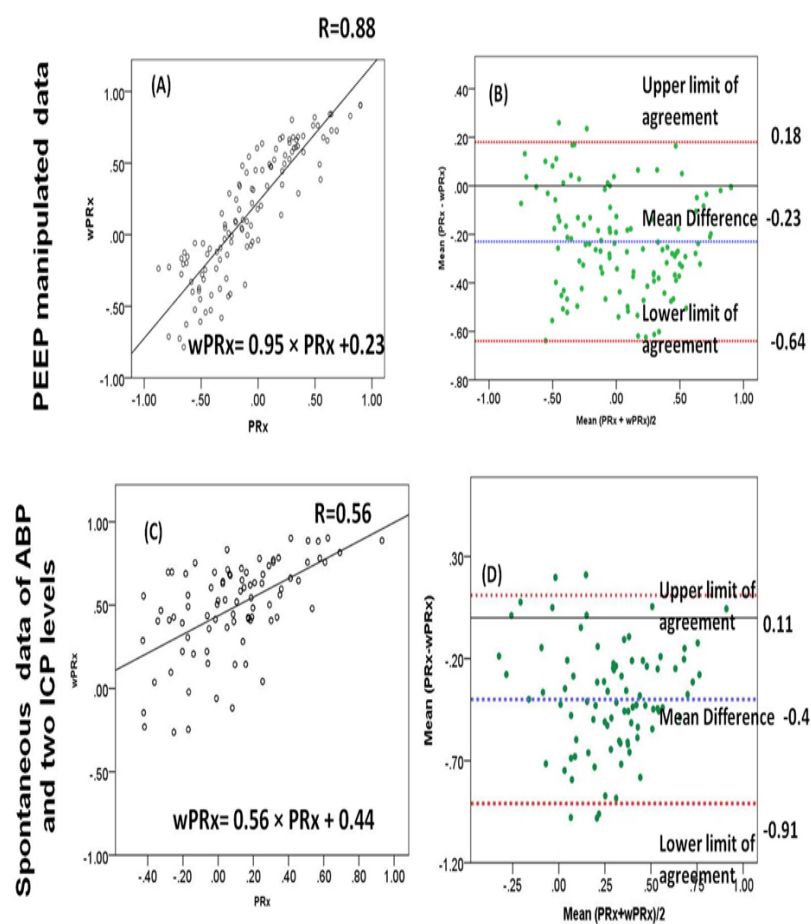


Fig.4 Comparison of PRx and wPRx against a standard LLA in PEEP group (data from one piglet). (A) An example of ABP, ICP, PRx and wPRx along continuous ABP decrease.

Cerebral autoregulation indices are binned in 5 mmHg increments of CPP for comparison against the LLA: (B) PRx, (C) wPRx. Positive CPP-LLA value is related with intact CA, and negative CPP-LLA implies impaired CA. PRx: pressure reactivity index; wPRx, wavelet pressure reactivity index, cosine of wavelet phase shift between arterial blood pressure and intracranial pressure, using wavelet coherence as threshold. Analyzed frequency was 0.0067 – 0.05 HZ. LLA: lower limit autoregulation.

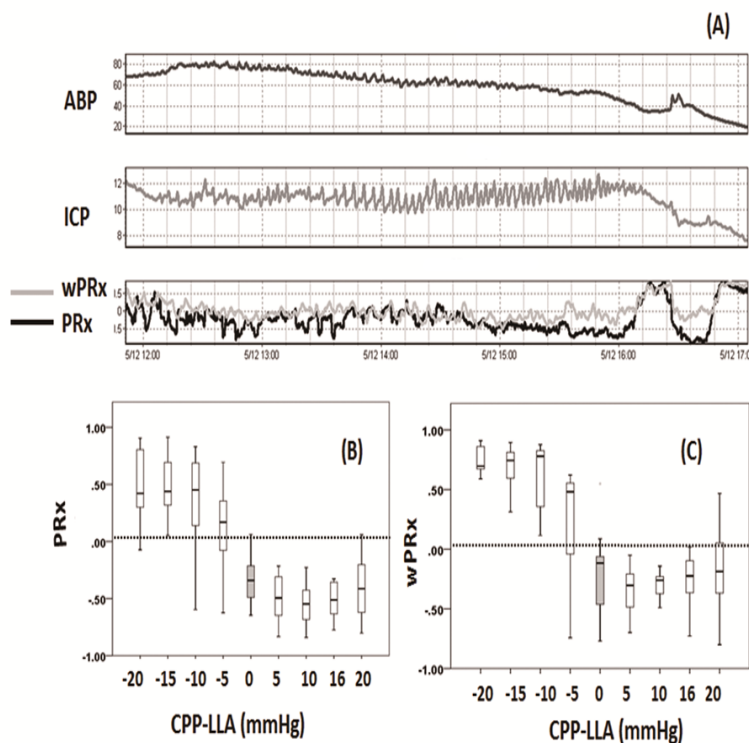


Fig.5 Performance of PRx and wPRx in distinguishing CPP above LLA and below LLA.

$P < 0.05$ implies significant difference. The white color bar implies PRx result; the stripe bar refers to wPRx result. Error bar: standard error. PRx: pressure reactivity index; wPRx: wavelet semblance; ICP, intracranial pressure; CPP, cerebral perfusion pressure; LLA, lower limit of autoregulation; CA: cerebral autoregulation.

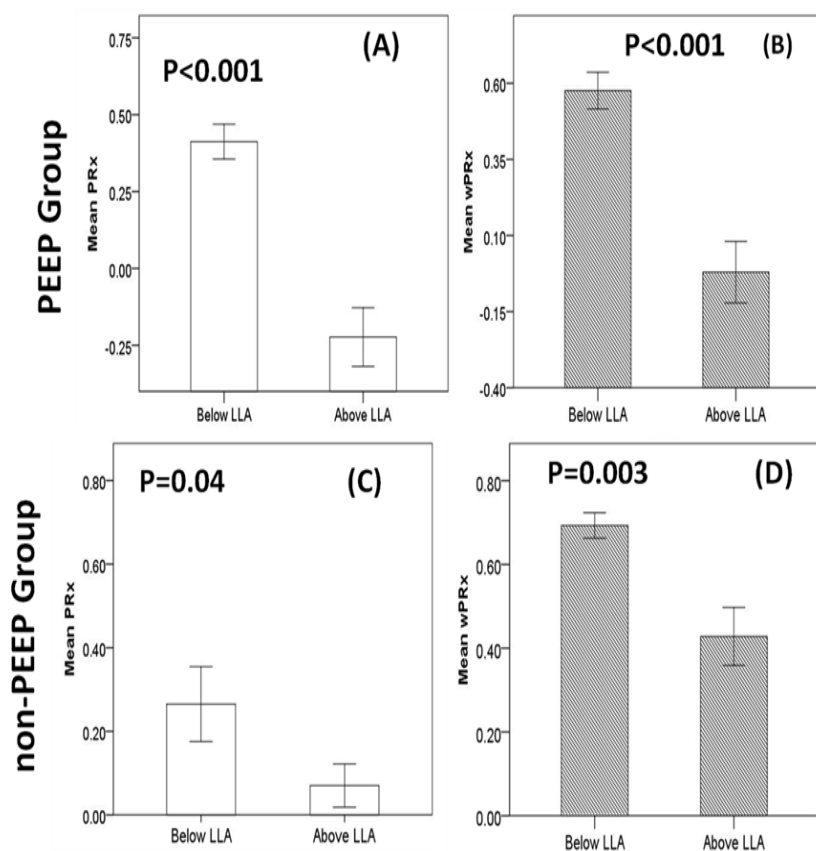


Fig.6 DeLong's test to compare the two AUC-ROC curves of PRx and wPRx in distinguishing CPP above LLA and below LLA in (A) PEEP group and (B) non-PEEP group. The area under the curve is where a value of 1 indicates maximum sensitivity and specificity. CA: cerebral autoregulation; PEEP: positive end-expiratory pressure. AUC-ROC: Area under a receiver-operator characteristic (ROC) test. LLA: lower limit of autoregulation.

